Materials Science and Engineering C 49 (2015) 472–484

Contents lists available at ScienceDirect

Materials Science and Engineering C

journal homepage: www.elsevier.com/locate/msec

Biocompatibility and drug release behavior of scaffolds prepared by coaxial electrospinning of poly(butylene succinate) and polyethylene glycol

E. Llorens [a], H. Ibañez [a], L.J. del Valle [a,*], J. Puiggalí [a,b]

[a] Departament d'Enginyeria Química, Universitat Politècnica de Catalunya, Av. Diagonal 647, Barcelona E-08028, Spain
[b] Center for Research in Nano-Engineering (CrNE), Universitat Politècnica de Catalunya, Edifici C, C/Pasqual i Vila s/n, Barcelona E-08028, Spain

ARTICLE INFO

Article history:
Received 18 July 2014
Received in revised form 19 December 2014
Accepted 7 January 2015
Available online 9 January 2015

Keywords:
Scaffolds
Coaxial electrospinning
Poly(butylene succinate)
Poly(ethylene glycol)
Drug release

ABSTRACT

Scaffolds constituted by electrospun microfibers of poly(ethylene glycol) (PEG) and poly(butylene succinate) (PBS) were studied. Specifically, coaxial microfibers having different core–shell distributions and compositions were considered as well as uniaxial micro/nanofibers prepared from mixtures of both polymers. Processing conditions were optimized for all geometries and compositions and resulting morphologies (i.e. diameter and surface texture) characterized by scanning electron microscopy. Chemical composition, molecular interactions and thermal properties were evaluated by FTIR, NMR, XPS and differential scanning calorimetry. The PEG component of electrospun fibers could be solubilized by immersion of scaffolds in aqueous medium, giving rise to high porosity and hydrophobic samples. Nevertheless, a small amount of PEG was retained in the PBS matrix, suggesting some degree of mixing. Solubilization was slightly dependent on fiber structure; specifically, the distribution of PEG in the core or shell of coaxial fibers led to higher or lower retention levels, respectively. Scaffolds could be effectively loaded with hydrophobic drugs having antibacterial and anticarcinogenic activities like triclosan and curcumin, respectively. Their release was highly dependent on their chemical structure and medium composition. Thus, low and high release rates were observed in phosphate buffer saline (SS) and SS/ethanol (30:70 *v*/*v*), respectively. Slight differences in the release of triclosan were found depending on fiber distribution and composition. Antibacterial activity and biocompatibility were evaluated for both loaded and unloaded scaffolds.

© 2015 Elsevier B.V. All rights reserved.

1. Introduction

Electrospinning is currently one of the simplest methods of drug loading into micro/nanofiber scaffolds. The drug is dissolved or dispersed in a polymer solution that is subsequently exposed to a strong electrical potential. Electrical charges accumulate on the surface of a liquid droplet placed at the tip of a capillary and a charged jet is ejected towards a grounded electrode when the Coulombic repulsion of the charges overcomes the surface tension of the polymer droplet [1–4]. The solvent evaporates as it travels from the tip to the grounded target and fibers with different morphologies are collected depending on solution properties (viscosity, dielectric constant, volatility, concentration, etc.) and operational parameters (strength of the applied electric field, deposition distance, flow rate, etc.) [5,6].

Electrospun scaffolds for tissue regeneration and drug delivery applications have been successfully prepared from both natural polymers like collagen, gelatin, chitosan, silk fibroin and hyaluronic acid and synthetic homopolymers and copolymers such as poly(lactic acid) (PLA), poly(ε-caprolactone) (PCL), polyethylene glycol (PEG), poly(butylene succinate), poly (L-lactide-*co*-caprolactone) and poly(lactic-*co*-glycolic acid) (PLGA) [7–11].

Drug-loaded micro/nanofiber scaffolds can be applied topically or as an implant for antibiotic, antifungal, antimicrobial [12], antioxidant [13] and anticancer [14] drug delivery. Despite the simplicity of the encapsulation procedure based on electrospinning, some requirements should be met to attain optimal results. Thus, release behavior becomes highly dependent on the distribution of drug molecules in electrospun fibers, as well as on the final morphology of fibers. Physicochemical interactions between drug molecules and the polymer matrix play a fundamental role, and specifically the hydrophobic–hydrophilic properties of drug and polymer should be matched to achieve good drug encapsulation inside electrospun nanofibers. Lack of good interactions may cause drug migration during electrospinning on or near the fiber surface, resulting in a significant burst effect [15]. In order to achieve sustained release and improve molecular interactions, blending hydrophilic–hydrophobic polymers in different ratios have been considered [16,17].

Coaxial electrospinning is a modification of the classical procedure that enables production of micro/nanofibers with a core–shell structure and highly different compositions. In this case, two

* Corresponding author.
E-mail address: luis.javier.del.valle@upc.edu (L.J. del Valle).

http://dx.doi.org/10.1016/j.msec.2015.01.039
0928-4931/© 2015 Elsevier B.V. All rights reserved.

polymer solutions are supplied by means of two separate syringe pumps and pipelines leading to a core–shell nozzle. At the exit of this special needle a core–shell droplet appears and acquires a shape similar to the Taylor cone. Nevertheless, the core material may be not entrained into the shell jet, giving rise to monolithic instead of core–shell jets [18]. In fact, electric charges escape very rapidly to the outer surface of the forming jet and core entrainment becomes only possible by viscous tractions [19]. Successful encapsulation of drug into the core of coelectrospun fibers is determined by various parameters (e.g. shell polymer concentration, core polymer concentration, molecular weight and drug concentration) as well as the relative flow rate of the core and shell solutions [20]. Fiber morphology is sometimes critical and incorporation of a highly hydrophilic and water soluble PEG polymer may accelerate transport of drug molecules into the environment [20]. Coaxial electrospun nanofibers have gained much interest as gene- and growth factor-delivery systems, as well as embedding media of pharmaceutical compounds such as antibiotic or antioxidant drugs [21,22].

PEG is a highly hydrophilic polymer widely used in the biomedical field because of its lack of toxicity, good biocompatibility and easy elimination from the human body [23]. Polybutylene succinate (PBS), a polymer supplied by Showa High Polymers as Bionolle™ is currently the most commonly employed poly(alkylene dicarboxylate) due to its relatively low production cost, good thermal and mechanical properties and easy processability [24,25]. To the best of our knowledge, no studies have been performed on the preparation of coaxial core–shell structures constituted by these two biocompatible polymers with well-differentiated hydrophilic–hydrophobic properties.

Triclosan (polychlorophenoxy phenol) (Fig. 1) is a well-known antibacterial and antifungal agent [26] scarcely soluble in water but well soluble in ethanol. At in-use concentrations, triclosan acts as a biocide, with multiple cytoplasmic and membrane targets [26]. At lower concentrations, however, triclosan appears bacteriostatic and is seen to target bacteria mainly by inhibiting fatty acid synthesis. Curcumin is a molecule constituted by two phenol groups connected by α,β-unsaturated carbonyl groups (Fig. 1). These diketones can form stable enols and are readily deprotonated to form enolates. Curcumin seems to have beneficial effects on various diseases, including multiple myeloma, pancreatic cancer, myelodysplastic syndromes, colon cancer, psoriasis, and Alzheimer's disease [27,28]. Curcumin is also a pleiotropic molecule capable of interacting with molecular targets involved in inflammation.

The main goal of the present work is the study of scaffolds constituted by PEG and PBS microfibers. To this end, electrospinning will be performed using a solution mixture of both polymers and compared with coaxial electrospinning having both PEG–PBS and PBS–PEG core–shell distributions. Morphological changes caused by rapid solubilization of PEG in aqueous media will also be evaluated since PEG can be used as a sacrificial polymer to modify material porosity and cell colonization. Finally, scaffolds will be studied as drug delivery systems considering the loading of triclosan and curcumin drugs in PEG and PBS components, respectively. This distribution should probably lead to a fast release of PEG taking into account its solubilization in aqueous media, and consequently to an immediate antibactericidal effect. On the contrary, loading of curcumin in the non-soluble polymer should result in a slower release rate, and therefore in a sustained anticancer effect. Basically, the new process may be interesting to load drug with highly different characteristics and may bring an opportunity to get a different release for the loaded drugs.

2. Materials and methods

2.1. Materials

Poly(ethylene glycol) samples of number average molecular weight of 35,000 g/mol were purchased from Sigma-Aldrich. Polybutylene succinate is a commercial product (Bionolle® 1001) supplied by Showa Denko K.K. (Germany). The polymer has a melt flow index of 1.6 g/10 min (measured at 190 °C under a load of 2.16 kg according to ASTM-D1238). The coaxial electrospinning apparatus was purchased from Linari Engineering SRL (Italy). Solvents, curcumin, triclosan and cell culture labware were purchased from Sigma-Aldrich (USA). *Escherichia coli* CECT 101 and *Micrococcus luteus* CECT 245 bacterial strains were obtained from the Spanish Collection of Type Culture (Valencia, Spain). Fibroblast-like MRC-5 and African green monkey kidney epithelial (Vero) cells were purchased from ATCC (USA).

2.2. Electrospinning

Electrospun fibers were collected on a target placed at different distances (10–25 cm) from the needle tip (inside diameter 0.84 mm) or the core–shell nozzle (inside diameters 1.37 mm and 2.39 mm) for single fiber or core–shell structure preparations, respectively. The voltage was varied between 10 and 30 kV and applied to the target using a high-voltage supply (Gamma High Voltage Research, ES30-5W). Polymer solutions were delivered via a single or two KDS100 infusion syringe pumps (KD Scientific, USA) to control the flow rate (from 1 to 5 mL/h). All electrospinning experiments were carried out at room temperature. Unloaded and triclosan and curcumin loaded electrospun

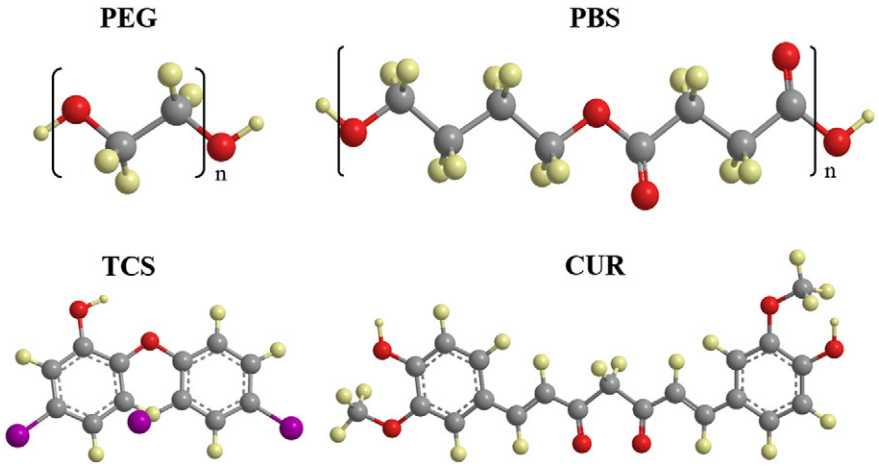

Fig. 1. Chemical structures of polymers (PEG and PBS) used to prepare coaxial electrospun microfibers and loaded drugs, triclosan (TCS) and curcumin (CUR).

Table 1
Optimal electrospinning conditions for the electrospinning of PBS/PEG microfibers.

Fiber	PBS/PEG (feed)[a]		Voltage (kV)	Flow rate (mL/h)	Diameter (μm)	PBS/PEG (fiber)[b] (mol/mol)
	(*w*/*w*-%)	(mol/mol)				
PBSs/PEGc	5/10	14.9/85.1	20	5	4.20 ± 0.92	13.4/86.6
	7/10	19.6/80.4	20	2.5	2.76 ± 0.42	19.6/80.4
	5/15	10.4/89.6	15	1.2	3.37 ± 0.64	8.7/91.3
PBSc/PEGs	5/10	14.9/85.1	25	3	1.82 ± 0.27	10.5/89.5
	7/10	19.6/80.4	25	5	1.96 ± 0.32	14.4/85.6
	5/15	10.4/89.6	20	5	4.83 ± 1.27	8.1/91.9
PBS/PEG	5/10	14.9/85.1	25	4	0.43 ± 0.10	12.9/87.1
	7/10	19.6/80.4	25	2	0.75 ± 0.18	14.8/85.2
	5/15	10.4/89.6	20	4	0.76 ± 0.18	11.2/88.8

[a] Tip–collector distance was always 14 cm.
[b] Composition determined by ^{1}H-NMR.

fibers were prepared using optimized parameters (i.e. collector distance, voltage and flow rate) and solvent conditions (i.e. polymer and drug concentrations). The triclosan and curcumin contents of the electrospinning solutions were 1 and 0.5 *w*/*v*-% for samples used for release and antibacterial assays, and for cytotoxicity assays, respectively. Coaxial electrospun microfibers will be denoted by subscripts s and c, which indicate the polymer that constitutes the shell and the core, respectively. The absence of these subscripts indicates fibers were prepared from a polymer mixture. Weight percentages of each polymer in the electrospinning solutions are also given in the sample abbreviation.

2.3. Morphology, composition and properties of electrospun scaffolds

Optical microscopy studies were performed with a Zeiss Axioskop 40 microscope. Micrographs were taken with a Zeiss AxiosCam MRC5 digital camera.

Detailed inspection of texture and morphology of electrospun samples was conducted by scanning electron microscopy using a Focus Ion Beam Zeiss Neon 40 instrument (Carl Zeiss, Germany). Carbon coating was accomplished by using a Mitec K950 Sputter Coater fitted with a film thickness monitor *k*150x. Samples were visualized at an accelerating voltage of 5 kV. The diameter of electrospun fibers was measured with the SmartTiff software from Carl Zeiss SMT Ltd. For the latter, the diameters of 100 fibers were measured, and values were analyzed using a frequency distribution adjusted to Gaussian model using the OriginPro v10 software (Origin Microcal, USA).

^{1}H-NMR spectra were acquired with a Bruker AMX-300 spectrometer operating at 300.1 MHz. Chemical shifts were calibrated using tetramethylsilane (TMS) as an internal standard. Deuterated chloroform ($CDCl_3$) was used as the solvent at room temperature.

Infrared absorption spectra were recorded in the 3600–600 cm^{-1} range on a Jasco FTIR 4100 Fourier Transform infrared spectrometer. A Specac MKII Golden Gate attenuated total reflection (ATR) accessory was employed.

X-ray photoelectron spectroscopy (XPS) was performed with a SPECS system equipped with an Al anode XR50 source operating at 200 W and a Phoibos 150 MCD-9 detector XP. Samples were fixed in a special sample holder with double sided carbon adhesive tape. The overview spectra were recorded with pass energy of 25 eV at 0.1 eV steps at a pressure below 7.5×10^{-9} mbar, with binding energies being referred to the C1s and O1s signals. The overlapping peaks were deconvoluted using the PeakFit v4 program by Jandel Scientific Software.

Contact angles (CA) were measured at room temperature with sessile drops using an OCA-15 plus Contact Angle Microscope (Dataphysics, USA) and SCA20 software. Contact angle values of the right and left

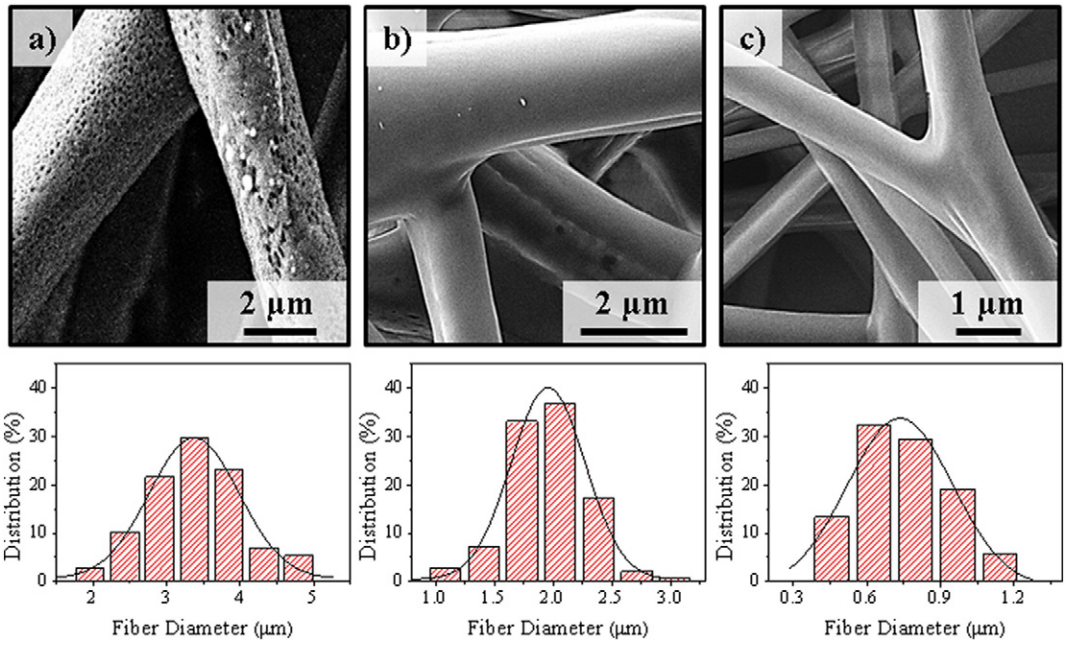

Fig. 2. SEM micrographs showing the texture of representative PBSs/PEGc 5/15 (a), PBSc/PEGs 7/10 (b) and PBS/PEG 7/10 (c) samples obtained from dichloromethane solutions under optimized concentration conditions of voltage needle–collector distance and flow. Diameter distribution of fibers for each electrospun samples (bottom).

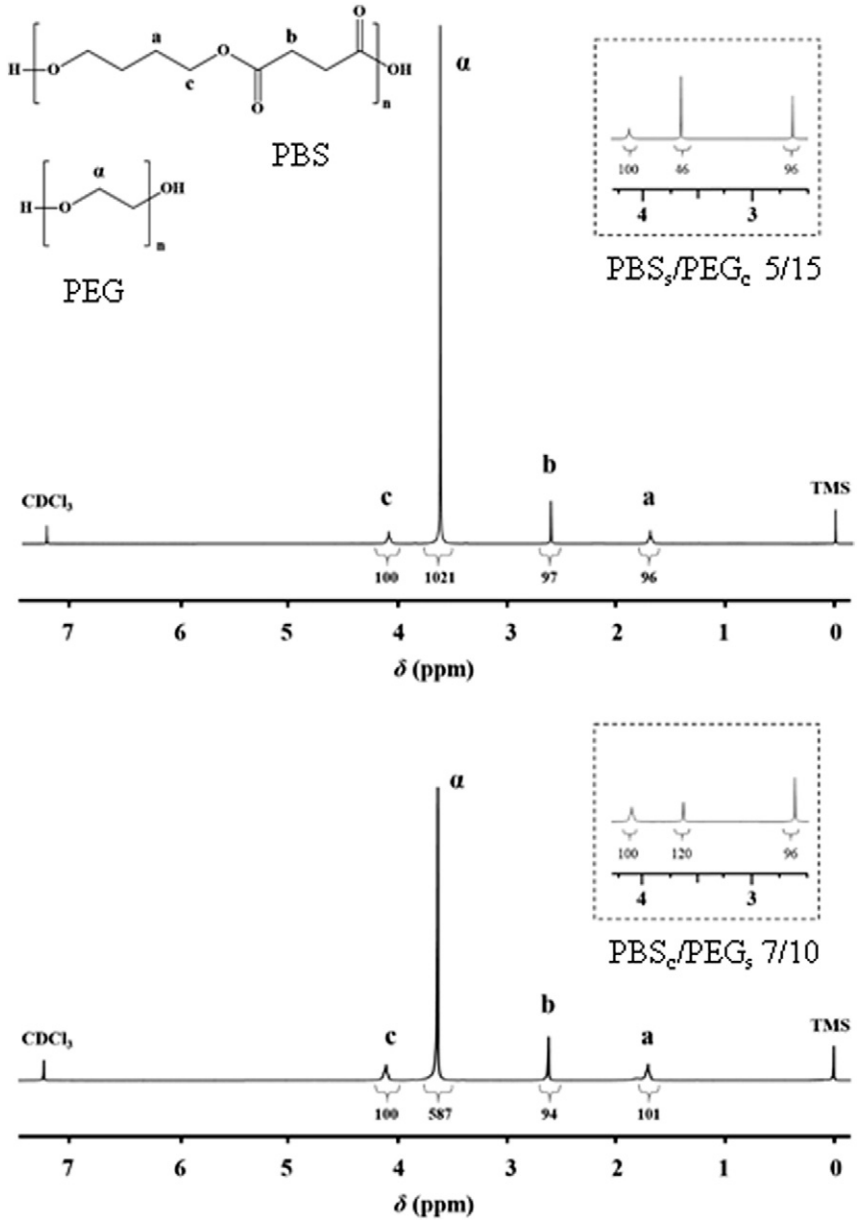

Fig. 3. [1]H-NMR spectra of PBSs/PEGc 5/15 (top) and PBSc/PEGs 7/10 (bottom) electrospun samples before and after immersion in water (insets).

sides of distilled water drops were measured and averaged. Measurements were performed 10 s after the drop (5 mL) was deposited on the sample surface. All CA data were an average of six measurements on different surface locations.

Calorimetric data were obtained by differential scanning calorimetry with a TA Instruments Q100 series equipped with a refrigeration cooling system (RCS). Experiments were conducted under a flow of dry nitrogen with a sample weight of approximately 5 mg, and calibration was performed with indium. Heating and cooling runs were carried out at rates of 20 °C/min and 10 °C/min, respectively.

2.4. Water uptake of scaffolds

The water uptake of electrospun scaffolds was measured by the liquid intrusion method. Vacuum dried scaffolds ($n = 3$) were weighed prior to immersion in water for 1 h using a shaker table to allow diffusion of water into the void volume. The scaffolds were taken out and reweighed. In this procedure a minimum value for the porosity was calculated according to Eq. (1) since the solubilized PEG fraction was not considered in the denominator:

$$P = [(m_w - m_d)/d_s]/\left\{[(m_w - m_d)/d_s] + \left[m_d^{PBS}/d_{PBS}\right] + \left[m_d^{PEG}/d_{PEG}\right]\right\} \quad (1)$$

where m_w, m_d, m_d^{PBS}, and m_d^{PEG} are the weights of the wet scaffold, dry scaffold, PBS fraction and PEG fraction in the dry scaffold, respectively, and d_s, d_{PBS} and d_{PEG} refer to the densities of water (1.0 g/mL), semicrystalline PBS (1.26 g/mL) and semicrystalline PEG (1.07 g/mL), respectively. The last two densities were estimated using DSC data of scaffolds which pointed to high crystallinity for both PBS and PEG phases.

2.5. Removal of PEG from scaffolds

PEG component of electrospun fibers was solubilized by water immersion of scaffolds. Square pieces of 20 mg were incubated in 50 mL of water milliQ under overnight agitation (200 rpm) at 37 °C. Then,

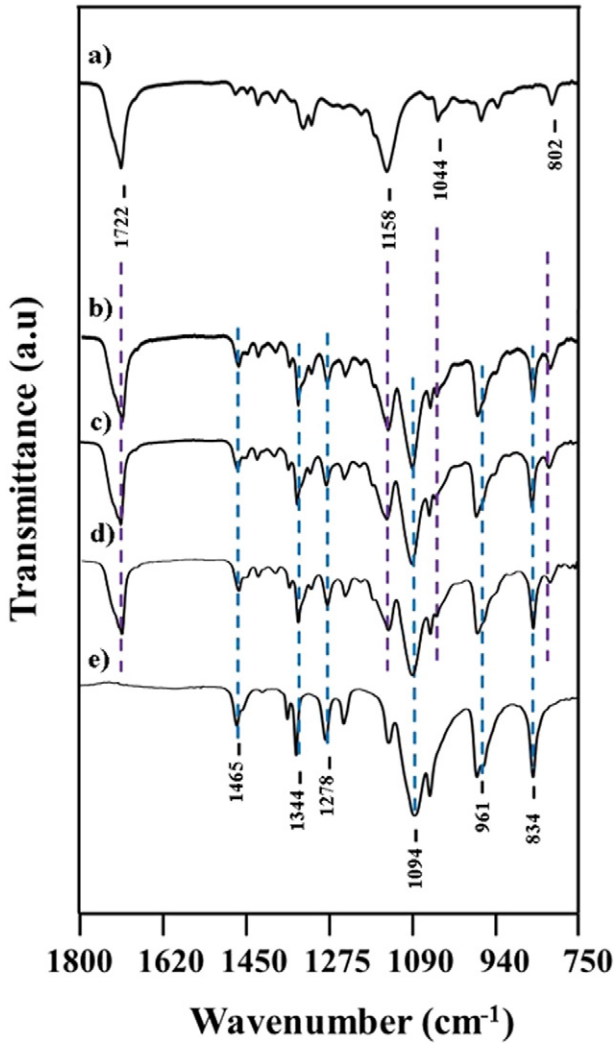

Fig. 4. FTIR spectra of PBS (a), PBSs/PEGc 5/15 (b), PBSc/PEGs 5/15 (c), PBS/PEG 5/15 (d) and PEG (e) electrospun samples.

the scaffolds were dried in vacuum until constant weight. Finally, the samples were studied as indicated above (see Sections 2.3 and 2.4).

2.6. Release experiments

Controlled release measurements were made with square pieces (weighing approximately 20 mg) of the electrospun scaffolds which were incubated at 37 °C in an orbital shaker at 200 rpm in tubes of 50 mL for 1 week. Phosphate buffer saline (SS) and alternatively its mixture with ethanol (i.e. 3:7 *v*/*v* ratio) as a more hydrophobic component were employed as release media. Drug concentration was evaluated by UV spectroscopy using a Shimadzu 3600 spectrometer. Calibration curves were obtained by plotting the absorbance measured at 290 and 243 nm versus triclosan and curcumin concentrations, respectively, in the hydrophilic medium, whereas 280 nm was considered for triclosan when ethanol was added to the medium. Samples were withdrawn from the release medium at predetermined time intervals. The volume was kept constant by addition of fresh medium. All drug release tests were carried out using three replicates and the results were averaged.

2.7. Cell adhesion and proliferation assays

Human fetal lung fibroblast (MRC-5) and African green monkey kidney epithelial (Vero) cells were cultured in Dulbecco's Modified Eagle Medium (DMEM) as previously reported [29]. Square pieces ($0.5 \times 0.5 \times 0.1$ mm^3) of the electrospun scaffolds were placed into the wells of a multiwell culture plate. Samples were fixed with a small drop of silicone (Silbione® MED ADH 4300 RTV, Bluestar Silicones France SAS, Lyon, France) and then sterilized by UV-radiation in a laminar flux cabinet for 15 min. For the cell adhesion assay, aliquots of 50–100 μL containing 5×10^4 cells were seeded onto the electrospun samples in each well and incubated for 24 h (adhesion assay) or 4 days (proliferation assay).

Samples were evaluated by the standard adhesion and proliferation method [13] using three replicates and the results were averaged. Samples with adhered and grown cells on the mats were fixed with 2.5% *w*/*v* formaldehyde at 4 °C overnight. They were subsequently dehydrated and processed for observation by scanning electronic microscopy.

2.8. Antimicrobial test

Escherichia coli (*E. coli*) and *Micrococcus luteus* (*M. luteus*) bacteria were selected to evaluate the antimicrobial effect of triclosan and curcumin loaded electrospun fibers. The bacteria were previously grown aerobically to exponential phase in broth culture (5 g/L beef extract, 5 g/L NaCl, 10 g/L peptone, pH 7.2).

Growth experiments were performed on a 24-well culture plate. Square pieces ($0.5 \times 0.5 \times 0.1$ mm^3) of the electrospun scaffolds were placed into each well. Then, 1 mL of broth culture containing 10^3 CFU was seeded on the electrospun fiber mats. The cultures were incubated at 37 °C and agitated at 200 rpm. Aliquots of 50 μL were taken at predetermined time intervals for absorbance measurement at 650 nm in a plate reader. Thus, turbidity was directly related to bacterial growth.

Bacterial adhesion onto scaffolds was also determined. The culture media were aspirated after incubation and the material was washed once with distilled water. Then, 0.5 mL of sterile 0.01 M sodium thiosulfate was added to each well. After addition of 4 mL of broth culture, the plate was incubated at 37 °C and agitated at 200 rpm for 24 h. The bacterial number was determined as above indicated. All assays were conducted in triplicate and the results averaged.

3. Results and discussion

3.1. Electrospinning conditions

A common solvent like dichloromethane was chosen for both PEG and PBS polymers and the two drugs (triclosan and curcumin) because its solubility parameter (20.31 MPa$^{0.5}$) is close to those reported for PEG [30] and PBS [31] (around 20 MPa$^{0.5}$). Polymer concentration and operational parameters (voltage and flow) were selected to obtain continuous fibers and avoid formation of droplets and beads, while needle–collector distance could be fixed at a value of 14 cm for all samples. In this way, concentration of the high molecular weight PBS sample was limited to the 5–7 wt.% range due to the high viscosity of the final solution, whereas the low molecular weight PEG sample required a concentration of 10–15 wt.% to avoid formation of droplets.

The best experimental conditions, together with the average diameter of the electrospun fibers, are summarized in Table 1. In all cases, a unimodal narrow distribution was observed. Note that fibers prepared from a common solution had significantly smaller diameters than coaxial fibers (0.43–0.76 μm as opposed to 1.82–4.83 μm) due to differences in the size of corresponding needles. The diameters of coaxial microfibers seemed to increase with polymer concentration in the electrospinning solution when PEG was in the fiber shell, whereas an unclear trend was observed when it was in the core since, in this case, a higher variation in the processing parameter was required (i.e. flow rate changed from 5 to 1.2 mL/h). Logically, the increase in polymer concentration and the decrease in the flow rate lead to opposite effects.

SEM micrographs of representative samples allow comparing fiber surface textures for some representative samples (see Fig. 2). In general, a significant difference can be detected depending on

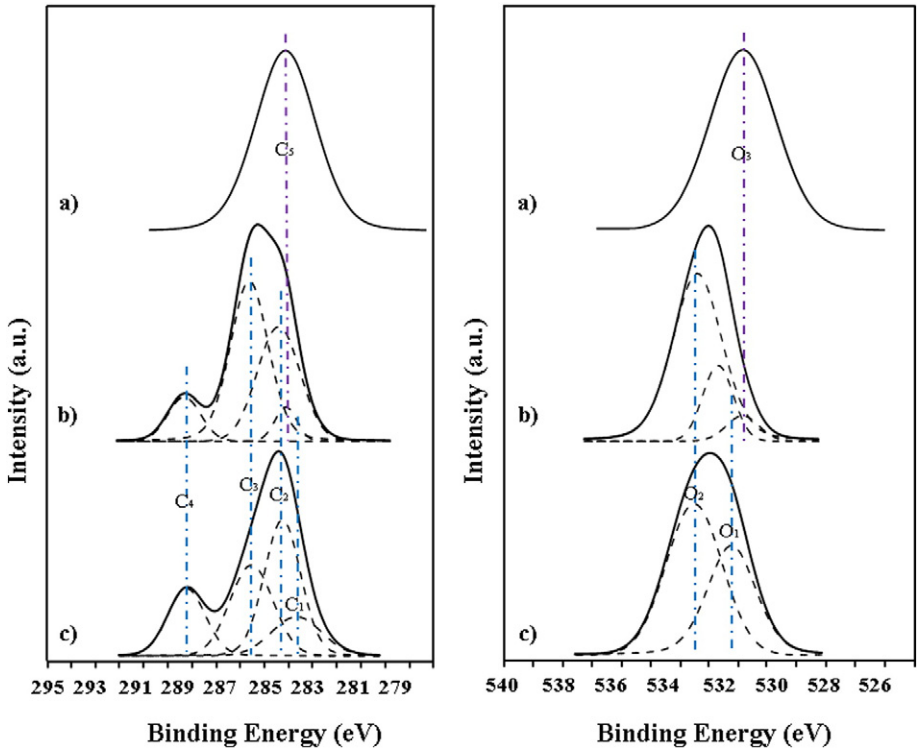

Fig. 5. Carbon (left) and oxygen (right) XPS signals of PEG (a), PBS/PEG 5/15 (b) and PBS (c) electrospun samples.

the polymer in the shell of the coaxial fiber. Thus, rough or smooth surfaces were characteristic of fibers having a PBS or PEG shell, respectively. Similarly, the narrowest nanofibers obtained from the polymer mixtures showed the smoothest surfaces, as is characteristic of PEG and also of mixtures with a high PEG content (e.g. higher than 55 wt.%) [32].

3.2. Composition and properties of PBS/PEG electrospun fibers

^{1}H-NMR spectra (Fig. 3) were useful to determine the composition of all electrospun samples. Thus, areas corresponding to methylene protons of PBS (4.11, 2.62 and 1.70 ppm) and PEG (3.64 ppm) were used to determine the molar PBS content of electrospun fibers as follows (Eq. (2)):

$$\mathrm{PBS(M\text{-}\%)} = 100 \cdot \left(\frac{A_{4.11} + A_{2.62} + A_{1.70}}{12}\right) \Big/ \left[\left(\frac{A_{4.11} + A_{2.62} + A_{1.70}}{12}\right) + \left(\frac{A_{3.64}}{4}\right)\right]. \quad (2)$$

Composition values summarized in Table 1 show relatively good agreement with the polymer molar feed ratio in the initial electrospinning solutions. In particular, it was excellent for the coaxial fibers having PEG confined in their core, whereas a slight deficiency was detected in PEG when it was the component of the shell jet. An unclear trend was observed for uniaxial fibers but again PEG content was slightly lower than expected, chiefly when the PBS/PEG ratio increased.

FTIR spectra of the electrospun fibers logically showed the characteristic peaks associated with PBS (e.g. 1722, 1158, 1044 and 802 cm^{-1}) and PEG (e.g. 961 and 834 cm^{-1}) (Fig. 4) with a variable intensity ratio that depended on the composition. The spectra merely corresponded to the superposition of homopolymer spectra since no band displacements indicative of new intermolecular interactions were detected.

On the contrary, XPS spectra were relevant, as shown in Fig. 5, because analysis of C1s and O1s peaks showed the establishment of interactions between PEG and PBS molecules in the electrospun fibers. The PBS spectrum was very complicated, as had already been reported [33], because four C1s and two O_1 peaks were found in the deconvoluted spectrum at 284.5 eV (C_1–CH_2), 285.2–285.6 eV (C_2–C═O), 286.4–286.9 (C_3–O), 289.3 eV (C_4═O), 531.6 eV (O_1═C) and 533.0 eV (O_2–C═O), whereas the PEG spectrum was characterized by single C1s and O1s peaks at binding energies of 285.0 eV (C_5–O) and 532.5 eV (O_3–C) [34]. Note in Fig. 5 that the spectrum of a representative PBS/PEG sample clearly differs from that expected from a weighted addition according to the final composition of the homopolymer spectra. Thus, for

Table 2
Selected calorimetric data from the heating and cooling scans performed with the different PBS/PEG electrospun samples.

Sample	PEG component				PBS component			
	T_m (°C)	ΔH_m ($J \cdot g^{-1}$)	T_c (°C)	ΔH_c ($J \cdot g^{-1}$)	T_m (°C)	ΔH_m ($J \cdot g^{-1}$)	T_c (°C)	ΔH_c ($J \cdot g^{-1}$)
PBS[a]	–	–	–	–	111.0	56.9	77.7	59.2
PBS	–	–	–	–	110.3	75.7	79.7	61.4
PEG[a]	65.0	177.2	44.4	177.2	–	–	–	–
PEG	63.8	176.1	44.7	175.7	–	–	–	–
PBSs/PEGc 5/10	56.9	90.4	37.7	80.5	109.1	27.5	78.6	30.0
PBSc/PEGs 5/10	62.3	125.3	34.6	111.7	106.5	17.7	76.3	19.2
PBS/PEG 5/10	62.5	121.3	34.3	103.5	111.7	28.1	79.4	26.4

[a] Pellets of the commercial sample.

Table 3
Diameter (mean ± SD) and composition of electrospun fibers after removal of PEG.

Sample	PBS/PEG (*w*/*w*-%)	Ø (μm)	ΔØ[a] (μm)	PBS/PEG[b] (mol/mol)	PEG_{rem}[c] (%)
PBSs/PEGc	5/10	2.39 ± 0.56	−1.81	55.0/45.0	87
	7/10	–	–	59.7/40.3	84
	5/15	1.67 ± 0.36	−1.70	45.0/55.0	88
PBSc/PEGs	5/10	1.51 ± 0.24	−0.31	59.8/40.2	92
	7/10	2.02 ± 0.30	–	68.8/31.2	92
	5/15	2.59 ± 0.94	−2.24	58.2/41.8	94
PBS/PEG	5/10	0.31 ± 0.08	−0.12	55.8/44.2	88
	7/10	0.54 ± 0.14	−0.21	58.0/42.0	87
	5/15	0.64 ± 0.29	−0.12	60.7/39.3	92

[a] Variation respect to the initial diameter (see Table 1).
[b] Molar percentage of PEG removed with respect to the initial PEG content.
[c] Composition determined by ^{1}H-NMR.

example, peak O_1 appeared shifted to a higher binding energy and the intensities of peaks O_3 and C_3 were lower and higher than expected, respectively.

Table 2 summarizes the main melting and crystallization data of electrospun samples, including data from the commercial pellets of the homopolymers. Several points merit attention: a) Crystallinity of electrospun PBS was higher than that of the commercial sample whereas similar crystallinities were attained after the cooling scan from the melt. Thus, melting enthalpies of 75.7 and 56.9 J/g were determined in the heating scans of electrospun and commercial PBS samples, whereas crystallization enthalpies of 61.4 and 59.2 J/g were determined in the corresponding cooling scans. Therefore, the electrospinning process seems to favor the orientation of PBS molecules and facilitate subsequent crystallization. b) Similar melting and crystallization enthalpies were determined for PEG commercial and electrospun samples. c) Characteristic PEG and PBS crystalline domains were observed in the DSC scans of electrospun PBS/PEG samples. Nevertheless, a slight decrease in the melting point was found for the component in the core of coaxial fibers (i.e. melting points of PEG and PBS decreased from 65 °C and 111 °C to 56.9 and 106.5 °C, respectively). This feature suggests that the polymer confined in the inner part of the microfiber had greater difficulty in forming more perfect and thicker lamellae as a consequence of significant retention of solvent or even a lower degree of orientation. d) Crystallization enthalpies associated with the PEG component in the binary electrospun samples were clearly lower than the corresponding melting enthalpies detected in the previous heating run (e.g. 103.5 and 121.3 J/g for PBS/PEG 5/10) whereas better agreement was found between crystallization and melting enthalpies of the PBS component. In the case of PEG, it is likely that its crystallization from the melt was hindered by constraints imposed by previous crystallization of the higher melting point PBS component.

3.3. Water solubility of PBS/PEG scaffolds

The high solubility of PEG in water allowed its use as a sacrificial polymer to increase the porosity of the scaffold after exposure to an aqueous medium. The solubilization of PEG in the different electrospun scaffolds can be evaluated through ^{1}H-NMR spectra for two different compositions and core–shell structures, as shown in Fig. 3. A clear decrease in the intensity of the typical PEG signal (3.64 ppm) was always observed after immersion of the samples in water. Final compositions deduced from NMR spectra are summarized in Table 3, together with the percentage of PEG compared to the initially solubilized content. Although these values were always high and around 90%, some significant amount of PEG was held in the PBS matrix (i.e. 31.2–55 M-%). Solubilization slightly depended on the fiber structure, and specifically the lowest and highest average percentages (87 and 94%) were found for coaxial fibers with PEG in the core and the shell, respectively, whereas an intermediate average value of 89% was determined for uniaxial fibers. The fact that no complete PEG removal was observed for the electrospun PBSc/PEGs sample suggests the formation of a non-perfect core–shell structure and some degree of mixing between both polymers, probably more significant in the interphase.

The morphology of microfibers was logically affected by solubilization of PEG for representative uniaxial and coaxial samples, as shown in Fig. 6. Thus, the smooth texture of uniaxial nanofibers became clearly rough (Fig. 6(a)) after immersion and their average diameter decreased between 29 and 39% of the initial value (Table 3), with the higher percentage being associated with fibers with an initially greater PEG content. Drastic changes occurred after immersion of coaxial PBSs/PEGc microfibers since longitudinal slits were usually observed (Fig. 6(b)). These slits could probably be a direct consequence of the release of the PEG component in the inner part of the fiber. Logically, the rough surface associated with the PBS shell remained after immersion. A significant diameter decrease was also observed, although in some cases no measurements could be performed due to the flat appearance of opened fibers. This percentage was obviously lower than that found for uniaxial fibers due to the greater diameter of coaxial fibers. Finally, PBSc/PEGs fibers exhibited a rough surface after the release of the PEG shell component (Fig. 6(c)) and a diameter decrease close to 17% comparable with that determined for

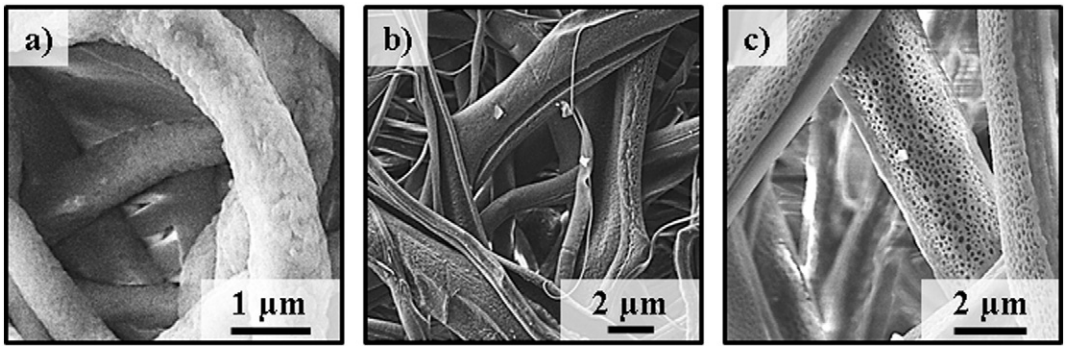

Fig. 6. High magnification SEM micrographs of PBS/PEG 5/15 (a), PBSs/PEGc 5/15 (b) and PBSc/PEGs 7/10 (c) electrospun samples after immersion in water.

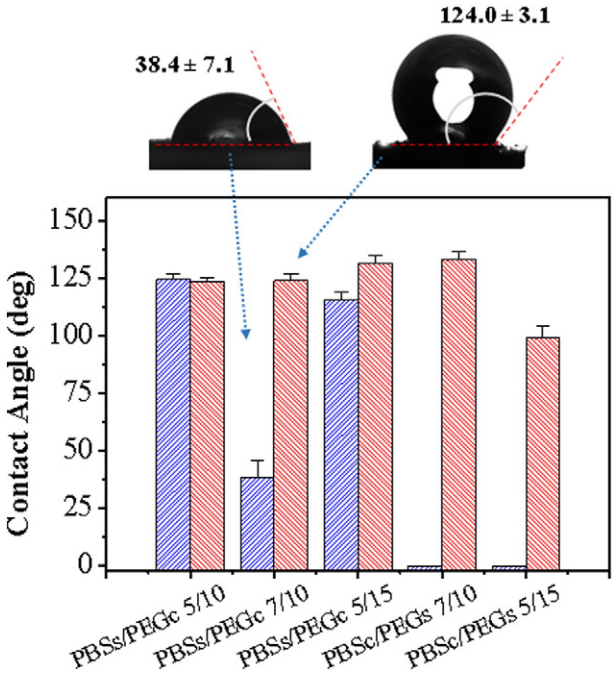

Fig. 7. Contact angles for PBSs/PEGc 5/10, 7/10 and 5/15 and PBSc/PEGs 7/10 and 5/15 scaffolds before (blue bars) and after (red bars) immersion in water. Inset shows the optical micrographs of a drop deposited on a representative scaffold.

PBSs/PEGc fibers with a similar initial diameter. Note in the given micrograph that PEG was still present in some parts of the fibers, giving rise to local smooth surfaces.

The water uptake was an estimation of the void volume of the porous scaffold. Thus, the determined values were high due to the solubilization of PEG. These were dependent on both the initial size of fibers and the distribution between the two components. Thus, lower porosities corresponded to PBSs/PEGc coaxial fibers (0.62–0.77) whereas maximum values (0.77–0.94) were determined for uniaxial nanofibers. It is interesting to note that the core–shell distribution played a significant role, and thus scaffolds derived from microfibers having a PEG shell had significantly higher porosity (0.71–0.88) than related ones having a PEG core. In the latter case, the external surface and probably the pore dimension of fibers should be less affected by solubilization.

3.4. Contact angle measurements

Information about the distribution of hydrophilic PEG and hydrophobic PBS in coaxial electrospun fibers can be verified through contact angle measurements, as shown in Fig. 7. The high hydrophilicity of PEG caused sessile drop spreading, and consequently angles could not be measured for any PBSc/PEGs sample. On the contrary, high contact angles were usually determined for PBSs/PEGc samples, indicating that PEG was well confined in the fiber core. Thus, values between 112° and 122° could be measured because of the correct core–shell structure, with hydrophobic PBS in the outer part of the fiber and the effective confinement of PEG. Note that only the PBSs/PEGc 7/10 sample had a non-perfect distribution or confinement since the contact angle decreased to 40°. In fact, measurements performed with melt pressed PBS films indicate a contact angle close to 90°, a value obviously lower than that determined for electrospun scaffolds because surface roughness is also a dominant factor in wettability of materials. The surface area of a rough surface is greater than the surface area of a comparably sized smooth surface, and consequently an increase of the contact angle should be expected [35]. The high increase of the contact suggests also that microfiber scaffolds benefit from air pocket formation [36]. Spreading was also characteristic for uniaxial fibers because of good mixing of polymers and the high PEG content.

Fig. 7 also compares contact angle measurements of scaffolds before and after immersion in water. Results clearly indicate that a hydrophobic PBS surface was attained after the removal of PEG, with the effect being more pronounced for PBSc/PEGs samples and even for the defective PBSs/PEGc 7/10 scaffold.

3.5. Drug load and release from PBS/PEG scaffolds

The micro/nanofibers of the studied samples were easily loaded with triclosan and curcumin by adding the appropriate amount of the drug in the corresponding electrospinning solution (i.e. triclosan in the PEG solution and curcumin in the PBS solution for coaxial fibers). Studies were performed with representative samples of the uniaxial and the two coaxial core/shell structures. Specifically, uniaxial fibers with the lowest and highest PEG content (i.e. PBS/PEG 5/15 and 7/10) were considered, together with the related coaxial samples with PEG in the core and the shell when its content was the highest and the lowest, respectively (i.e. PBSs/PEGc 5/15 and PBSc/PEGs 7/10). In this way, PBSs/PEGc 5/15 should have the fastest and the slowest release rate for curcumin and triclosan, respectively, while the opposite would be expected for PBSc/PEGs 7/10.

The incorporation of the drug had some influence on the electrospinning process, and consequently operational parameters were slightly modified, as indicated in Table 4. Conditions were also optimized to obtain similar sizes for the two kinds of coaxial fibers (i.e. 1.57–1.68 μm) as well as for the uniaxial fibers with different compositions (i.e. 0.68–0.77 μm). Fig. 8 shows the different textures attained with the drug loaded samples, which, as expected, corresponded to rough and smooth surfaces for the coaxial fibers with a PBS shell and the two uniaxial fibers, respectively. The only significant change was the appearance of transversal ribs in the coaxial sample with a PEG shell, in contrast with the smooth surface of the unloaded sample. Changes in fiber surface morphology may have played a significant role in supporting cell attachment but they did not when the polymer in the shell was highly soluble.

Immersion of loaded fibers in aqueous medium led to a decrease in the fiber diameter, a rough texture and solubilization of PEG (Table 4), with percentages of removed PEG being similar to those for unloaded samples.

Fig. 9 compares the release behavior of all scaffolds when they were exposed to a hydrophilic SS and to a more hydrophobic SS/ethanol

Table 4
Optimal electrospinning conditions applied for the selected drug loaded samples and resulting diameters before and after immersion in water.

Sample	Voltage (kV)	Rate (mL/h)	Distance (cm)	Ø[a] (μm)	Ø[b] (μm)	$PEG_{removed}$[c] (%)
PBSs/PEGc 5/15	25	1.35	17	1.57 ± 0.38	0.91 ± 0.22	83
PBSc/PEGs 7/10	25	4	24	1.68 ± 0.36	1.20 ± 0.26	94
PBS/PEG 5/15	20	2	14	0.68 ± 0.19	0.38 ± 0.08	91
PBS/PEG 7/10	20	1	14	0.77 ± 0.21	0.43 ± 0.10	92

[a] Before immersion in water.
[b] After immersion in water.
[c] Molar percentage of PEG removed by immersion in water with respect to the initial PEG content.

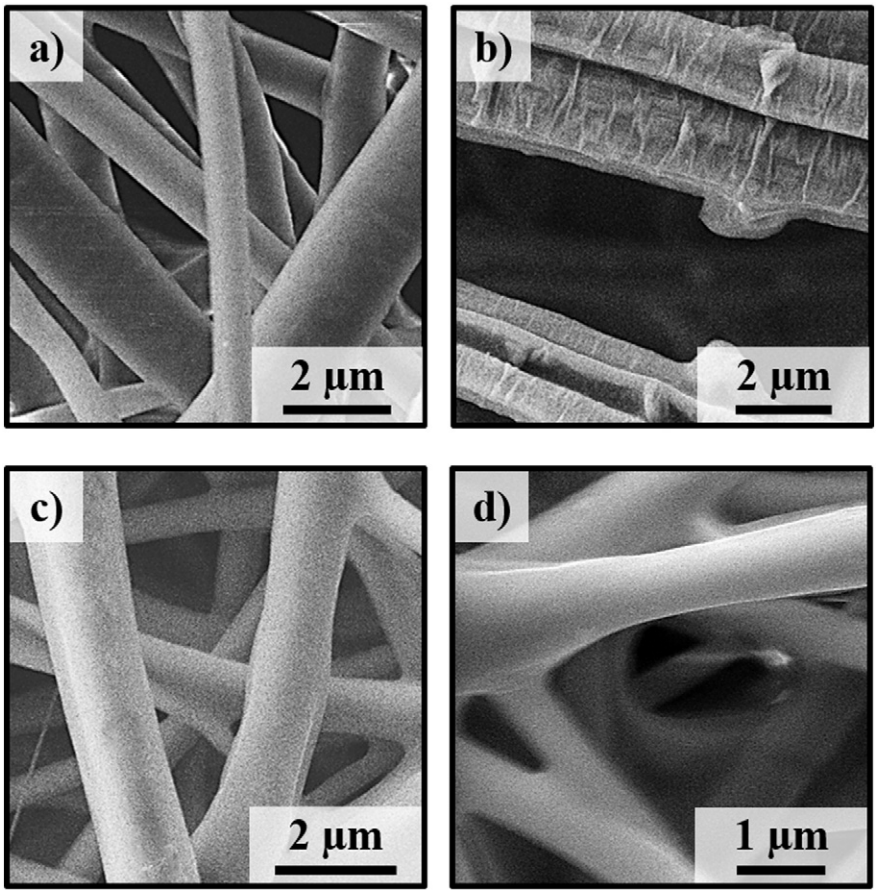

Fig. 8. High magnification SEM micrographs of drug loaded PBSs/PEGc 5/15 (a), PBSc/PEGs 7/10 (b), PBS/PEG 5/15 (c) and PBS/PEG 7/10 (d) scaffolds. Triclosan and curcumin were added in PEG and PBS solution, respectively.

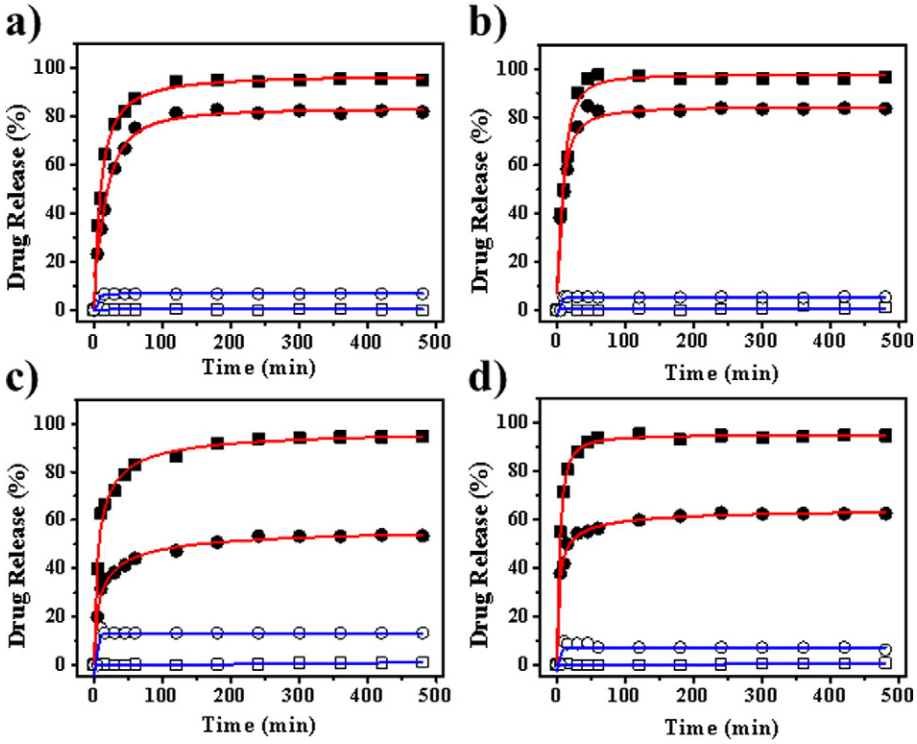

Fig. 9. Triclosan (circle) and curcumin (square) release curves in SS/ethanol mixture (30/70 *v*/*v*) (●, ■) and SS medium (○, □) for PBSs/PEGc 5/15 (a), PBSc/PEGs 7/10 (b), PBS/PEG 5/15 (c) and PBS/PEG 7/10 (d) scaffolds.

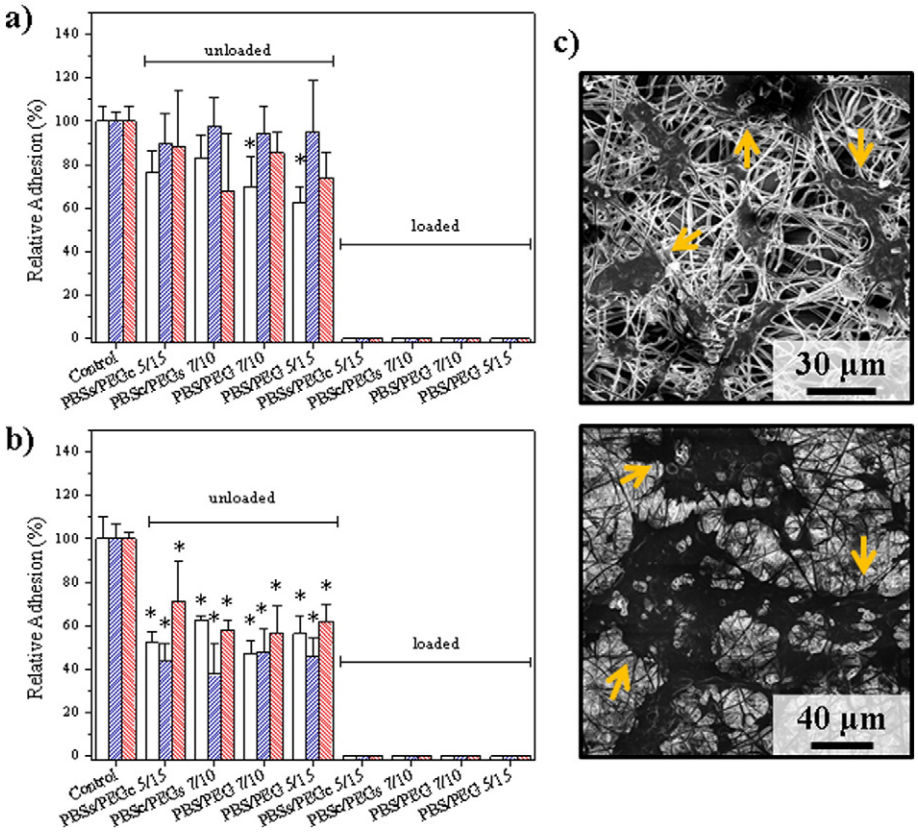

Fig. 10. Adhesion of MRC-5 (a) and Vero (b) cells on the control plate surface, selected scaffolds before (white bars) and after (blue bars) immersion in water and glutaraldehyde fixed scaffolds (red bars) (*$p < 0.05$ vs. control; ANOVA–Tukey's test). c) SEM micrographs showing adhesion of Vero cells (arrows) on PBSc/PEGs 7/10 scaffolds before (top) and after (bottom) immersion in water.

(30:70 *v*/*v*) mixture. Release proceeds at a similarly fast rate for all assayed samples until a limit value is reached. This value is highly dependent on the affinity between the drug and the release medium, and also varies with composition and structure of electrospun fibers. Some interesting features can be pointed out:

a) The amount of triclosan released in SS medium was low (i.e. between 5 and 13% of the loaded drug) and inferior to the solubility limit. Hence, this hydrophobic drug was effectively retained/adsorbed in the hydrophobic PBS component. It is remarkable that this adsorption was still found when the drug was only loaded in the water soluble PEG component in the shell of coaxial fibers. Somehow the drug moved towards the hydrophobic component in the inner part of fibers. The amount of released drug was higher for the thin uniaxial fibers and increased slightly with the PEG content (i.e. 14%, 9%, 7% and 5% for PBS/PEG 5/15 and PBS/PEG 7/10, PBSs/PEGc 5/15, PBSc/PEGs 7/10 samples, respectively).
b) The triclosan released in the medium containing ethanol was relatively high and strongly dependent on the fiber structure and composition. Therefore, the restriction of maximum amount of triclosan released was not due to limited solubility. Lower release percentages were found for uniaxial fibers (i.e. 52% and 62%, Fig. 9(c) and (d)) despite their lower diameter, probably as a consequence of the mixed arrangement of PEG and PBS in the fiber. Coaxial structures gave rise to a higher release that was similar for both distributions (i.e. 80% and 82% for fibers having PEG in the core and the shell, respectively, Fig. 9(a) and (b)).
c) The high difference between the release percentages of PBSs/PEGc 5/15 depending on the media (i.e. 7% and 82% for SS and SS/ethanol mixture, respectively) made it possible to discard an explanation based on a swelling effect of ethanol since triclosan was loaded into the PEG shell, which is soluble in both aqueous and ethanol solutions.

A minimum release of curcumin in SS medium was observed for all assayed samples (i.e. 1%) due to its high hydrophobicity and excellent interaction with PBS. This high retention was even observed for the thin uniaxial fibers where curcumin was loaded into the matrix constituted by the mixture of PEG and PBS polymers. On the contrary, curcumin was completely released independently of the fiber structure and composition in the medium containing 70 *v*-% of ethanol. Logically, a tuned release in function of the ethanol ratio in the media should be expected.

3.6. Biocompatibility of unloaded and triclosan loaded PLA/PEG scaffolds

Adhesion and proliferation of fibroblast MRC-5 and epithelial (Vero) cells were studied for all scaffolds. Both experiments are important to follow cell development since adhesion is an early cellular event whereas proliferation is an evidence of metabolic cell activity. Fig. 10(a) compares the results on relative adhesion for representative studied materials, which indicate that adhesion of fibroblast MRC-5 cells was well supported and even slightly improved when fibers were stabilized by solubilization of PEG or cross-linking with glutaraldehyde. On the other hand, epithelial cells were more sensitive and in general adhesion on studied scaffolds decreased by around 50% compared to the control (Fig. 10(b)).

Proliferation studies indicated that MRC-5 cells were able to colonize all materials without a statistical difference compared to the control (data not show); whereas colonization of Vero cells was proportional to their initial adhesion on the polymer scaffolds (see Fig. 11).

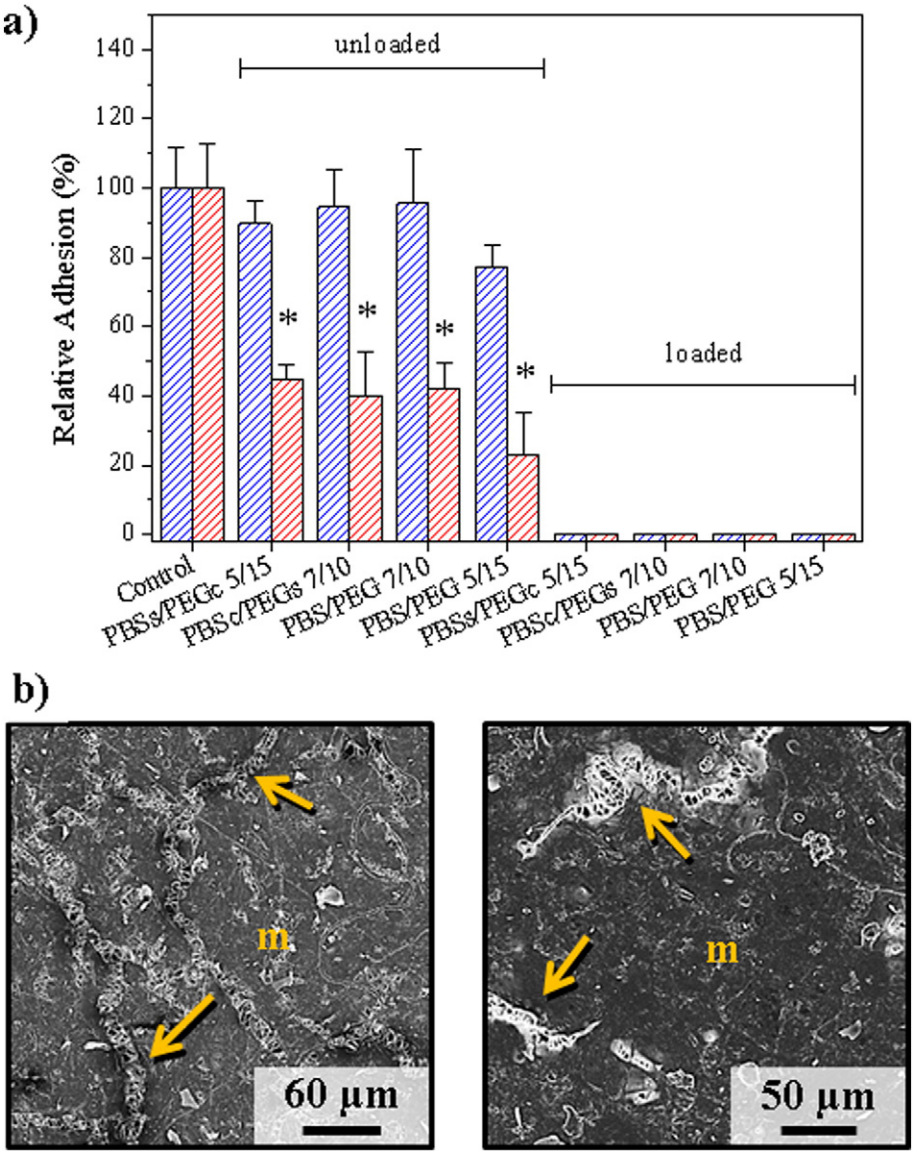

Fig. 11. (a) Proliferation of MRC-5 (blue bars) and Vero (red bars) cells on control plate surface and unloaded scaffolds (*$p < 0.05$ vs. control; ANOVA–Tukey's test). (b) SEM micrographs of Vero cells proliferation on representative PBSc/PEGs 7/10 (left) and PBS/PEG 7/10 (right) scaffolds. Arrows, point out electrospun fibers. m, cell monolayer.

SEM microscopy observations of cultures allowed the evaluation of morphological characteristics associated with cell adhesion and proliferation onto film surfaces (e.g. Figs. 10(c) and 11(b) for representative samples of Vero cells). Cells were attached and spread out on film surfaces after a seeding of 24 h, even for the more problematic Vero cells. These exhibited large areas of cytoplasm extending on the scaffold surfaces and promoting their attachment onto the material. Cells proliferated and reached confluence after 4 days of culture. Materials were effectively colonized, and specifically cells formed a monolayer with close contacts between them.

The adhesion and proliferation assays also reveal that the drug load necessary to perform the release experiments was too high to support both cell events. This means that both drugs were effectively released during culture and that minimum doses required to produce cell necrosis were always attained. Curcumin is an antitumor drug that is expected to reduce cell viability. The drug released from loaded matrices clearly showed a complete inhibition of cell viability as should expect from the specific activity of curcumin (i.e. the drug was effectively loaded and kept its activity). In fact, the cytotoxic concentrations of curcumin and triclosan required to reduce cell population by 50% (CC_{50}) were approximately 14–24 μg/mL and 6–15 μg/mL, respectively. The given intervals indicated the toxicity for the more sensitive Vero cells (lower values) and MRC-5 cells (higher values). Experimental cytotoxic concentrations were clearly lower than those calculated for complete release of loaded drugs (i.e. 50 and 100 μg/mL for curcumin and triclosan, respectively).

3.7. Antibacterial properties of triclosan loaded PLA/PEG scaffolds

Triclosan is a broad-spectrum antiseptic with documented safety and efficacy against Gram-positive and Gram-negative bacteria (e.g. *M. luteus* and *E. coli*, respectively). The antibacterial effect of triclosan released from scaffolds constituted by uniaxial and coaxial electrospun fibers was determined by studying bacterial adhesion and growth inhibition in broth medium.

As shown in Fig. 12 for unloaded samples, high adhesion of both bacteria was measured for all scaffolds. It was considerably greater than that measured for the control, probably as a consequence of the high specific surface and porosity of scaffolds. Therefore, it seems crucial to

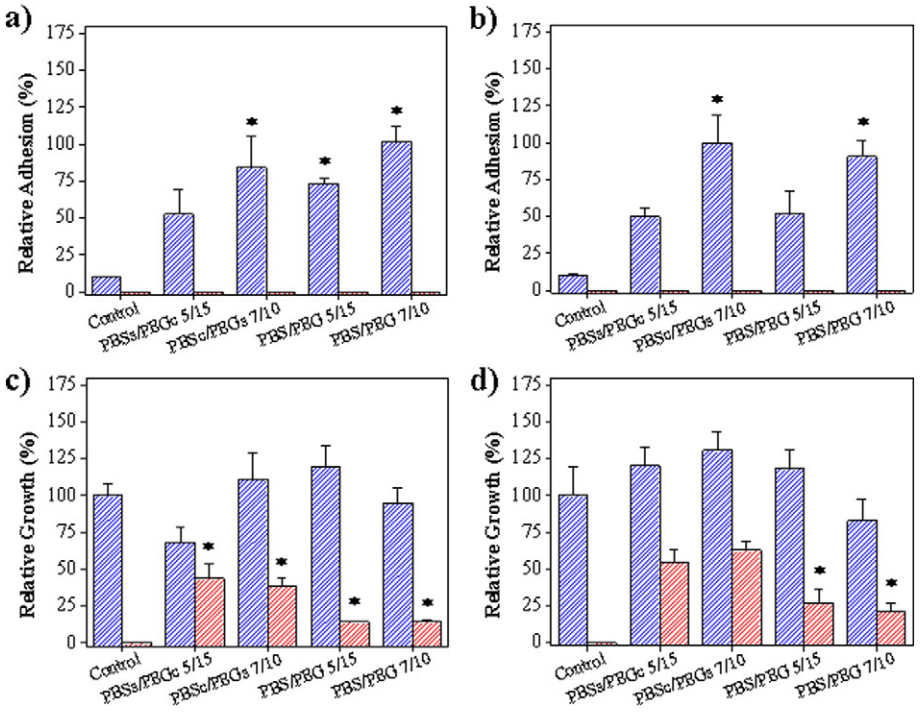

Fig. 12. Adhesion (a, b) and relative growth (c, d) of *Escherichia coli* (a, c) and *Micrococcus luteus* (b, d) on control surfaces and unloaded (blue bars) and TCS loaded (red bars) in PBSs/PEGc, PBSc/PEGs and PBS/PEG electrospun samples.

prevent bacterial colonization by means of an antiseptic, and in this sense triclosan was highly effective (Fig. 12(a)–(b)).

Growth inhibition measurements made with triclosan-loaded scaffolds (Fig. 12(c)–(d)) demonstrated that those constituted by coaxial fibers were more susceptible to colonization, whereas the core–shell structure had no significant influence. Thus, inhibitions between 60%–40% and 90%–75% were found for scaffolds constituted by coaxial and uniaxial fibers, respectively. These results agree qualitatively with the higher release observed for the thin uniaxial fibers in SS medium and demonstrated that the low release was sufficient to inhibit bacterial colonization. The effect of triclosan was clearly enhanced for the Gram-negative bacterium (i.e. *E. coli*) due to its higher sensitivity to the drug.

4. Conclusions

Coaxial microfibers with different core–shell distributions and constituted by PEG and PBS could be prepared from dichloromethane solutions and optimized processing parameters. These fibers had different surface textures depending on the polymer in the shell (i.e. smooth and rough for PEG and PBS, respectively), suggesting the success of coaxial electrospinning. This was also corroborated by contact angle measurements that demonstrated the hydrophilicity and hydrophobicity of coaxial fibers having a shell of PEG and PBS, respectively.

Calorimetric data indicated high crystallinity for PBS-rich domains caused by a molecular orientation favored by the electrospinning process. A decrease in the corresponding melting temperature also suggested that the polymer confined in the fiber core developed more defective crystals.

XPS spectroscopy revealed the establishment of new interactions between PBS and PEG in uniaxial nanofibers prepared from a common dissolution of both polymers. Thus, a significant amount of PEG remained in the scaffolds after immersion in water. This amount was dependent on fiber distribution, with higher and lower values being associated with coaxial fibers with a PBS shell and a PEG shell, respectively.

Release of triclosan and curcumin from loaded scaffolds was highly dependent on the media and their hydrophobicity. Slight differences were also detected depending on the structure of the fiber. Specifically, the lowest release was found for PEG-rich uniaxial nanofibers exposed to SS medium whereas the highest value corresponded to coaxial microfibers exposed to SS/ethanol mixture. Scaffolds constituted by coaxial microfibers were more susceptible to colonization by both Gram-positive and Gram-negative bacteria whereas the core–shell structure had no significant influence. Finally, the new matrices allow a fast release of the antimicrobial drug while a slow release was more appropriate for the antitumoral agent.

Acknowledgments

The authors are in debt to supports from MICINN-FEDER (MAT2012-36205) and the Generalitat de Catalunya (2009SGR1208).

References

[1] D.H. Reneker, I. Chun, Nanometre diameter fibres of polymer, produced by electrospinning, Nanotechnology 7 (1996) 216–223.
[2] A. Frenot, I.S. Chronakis, Polymer nanofibers assembled by electrospinning, Curr. Opin. Colloid Interface Sci. 8 (2003) 64–75.
[3] Y. Dzenis, Spinning continuous fibers for nanotechnology, Science 304 (2004) 1917–1919.
[4] K. Jayaraman, M. Kotaki, Y.Z. Zhang, X.M. Mo, S. Ramakrishna, Recent advances in polymer nanofibers, J. Nanosci. Nanotechnol. 4 (2004) 52–65.
[5] S.R. Dhakate, B. Singla, M. Uppal, R.B. Mathur, Effect of processing parameters on morphology and thermal properties of polycarbonate nanofibers, Adv. Mater. Lett. 1 (2010) 200–204.
[6] S. Sharma, Ferroelectric nanofibers: principle, processing and applications, Adv. Mater. Lett. 4 (2013) 522–533.
[7] M. Zamani, M.P. Prabhakaran, S. Ramakrishna, Advances in drug delivery via electrospun and electrosprayed nanomaterials, Int. J. Nanomedicine 8 (2013) 2997–3017.
[8] M. Spasova, O. Stoilova, N. Manolova, I. Rashkov, G. Altankov, Preparation of PLLA/PEG nanofibers by electrospinning and potential applications, J. Bioact. Compat. Polym. 22 (2007) 62–76.
[9] L.J. del Valle, R. Camps, A. Díaz, L. Franco, A. Rodríguez-Galán, J. Puiggalí, Electrospinning of polylactide and polycaprolactone mixtures for preparation of materials with tunable drug release properties, J. Polym. Res. 18 (2011) 1903–1917.
[10] E.H. Jeong, S.S. Im, J.H. Youk, Electrospinning and structural characterization of ultrafine poly(butylene succinate) fibers, Polymer 46 (2005) 9538–9543.
[11] Y. Liu, J.-H. He, J.-Y. Yu, Preparation and morphology of poly(butylene succinate) nanofibers via electrospinning, Fibres Text. East. Eur. 15 (2007) 30–33.

[12] X. Zong, S. Li, E. Chen, B. Garlick, K.S. Kim, D. Fang, J. Chiu, T. Zimmerman, C. Brathwaite, B.S. Hsiao, B. Chu, Prevention of postsurgery-induced abdominal adhesions by electrospun bioabsorbable nanofibrous poly(lactide-co-glycolide)-based membranes, Ann. Surg. 240 (2004) 910–915.
[13] E. Llorens, L.J. del Valle, A. Diaz, M.T. Casas, J. Puiggali, Polylactide nanofibers loaded with vitamin B_6 and polyphenols as bioactive platform for tissue engineering, Macromol. Res. 21 (2013) 775–787.
[14] R. Toshkova, N. Manolova, E. Gardeva, M. Ignatova, L. Yossifova, I. Rashkov, M. Alexandrov, Antitumor activity of quaternized chitosan-based electrospun implants against Graffi myeloid tumor, Int. J. Pharm. 400 (2010) 221–233.
[15] J. Zeng, L.X. Yang, Q.Z. Liang, X.F. Zhang, H.L. Guan, X.L. Xu, X.S. Chen, X.B. Jing, Influence of the drug compatibility with polymer solution on the release kinetics of electrospun fiber formulation, J. Control. Release 105 (2005) 43–51.
[16] K. Kim, Y.K. Luu, C. Chang, D. Fang, B.S. Hsiao, B. Chu, M. Hadjiargyrou, Incorporation and controlled release of a hydrophilic antibiotic using poly(lactide-co-glycolide)-based electrospun nanofibrous scaffolds, J. Control. Release 98 (2004) 47–56.
[17] H. Cao, X.G. Jiang, C.L. Chai, S.Y. Chew, RNA interference by nanofiber-based siRNA delivery system, J. Control. Release 144 (2010) 203–212.
[18] S.N. Reznik, A.L. Yarin, E. Zussman, L. Bercovici, Evolution of a compound droplet attached to a core–shell nozzle under the action of a strong electric field, Phys. Fluids 18 (2006) 062101.
[19] A.L. Yarin, Coaxial electrospinning and emulsion electrospinning of core–shell fibers, Polym. Adv. Technol. 22 (2011) 310–317.
[20] I.C. Liao, S. Chen, J.B. Liu, K.W. Leong, Sustained viral gene delivery through core–shell fibers, J. Control. Release 139 (2009) 48–55.
[21] C.L. He, Z.M. Huang, X.J. Han, L. Liu, H.S. Zhang, L.S. Chen, Coaxial electrospun poly(L-lactic acid) ultrafine fibers for sustained drug delivery, J. Macromol. Sci. Part B Phys. 45 (2006) 515–524.
[22] C.L. He, Z.-M. Huang, X.-J. Han, Fabrication of drug-loaded electrospun aligned fibrous threads for suture applications, J. Biomed. Mater. Res. A 89A (2009) 80–95.
[23] D.A. Herold, K. Keil, D.E. Bruns, Oxidation of polyethylene glycols by alcohol dehydrogenase, Biochem. Pharmacol. 38 (1989) 73–76.
[24] T. Fujimaki, Processability and properties of aliphatic polyesters, "BIONOLLE", synthesized by polycondensation reaction, Polym. Degrad. Stab. 59 (1998) 209–214.
[25] S.M. Lai, C.K. Huang, H.F. Shen, Preparation and properties of biodegradable poly(butylene succinate)/starch blends, J. Appl. Polym. Sci. 97 (2005) 257–264.
[26] A.D. Russell, Whiter triclosan? J. Antimicrob. Chemother. 53 (2004) 693–695.
[27] H. Hatcher, R. Planalp, J. Cho, F.M. Torti, S.V. Torti, Curcumin: from ancient medicine to current clinical trials, Cell. Mol. Life Sci. 65 (2008) 1631–1652.
[28] Y. Jiao, J. Wilkinson, X. Di, W. Wang, H. Hatcher, N.D. Kock, R. D'Agostino, M.A. Knovich, F.M. Torti, S.V. Torti, Curcumin, a cancer chemopreventive and chemotherapeutic agent, is a biologically active iron chelator, Blood 113 (2009) 462–469.
[29] S.C. Gupta, S. Prasad, J.H. Kim, S. Patchva, L.J. Webb, I.K. Priyadarsini, B.B. Aggarwal, Multitargeting by curcumin as revealed by molecular interaction studies, Nat. Prod. Rep. 28 (2011) 1937–1955.
[30] D. Karst, Y.Q. Yang, Using the solubility parameter to explain disperse dye sorption on polylactide, J. Appl. Polym. Sci. 96 (2005) 416–422.
[31] M. Imaizumi, T. Nagata, Y. Goto, Y. Okino, T. Takahashi, K. Koyama, Solubility parameters of biodegradable polymers form turbidimetric titrations, Kobunshi Ronbunshu 62 (2005) 438–440.
[32] E. Llorens, L.J. Valle, R. Ferrán, A. Rodríguez-Galán, J. Puiggalí, Scaffolds with tuneable hydrophilicity from electrospunmicrofibers of polylactide and poly(ethylene glycol) mixtures: morphology, drug release behavior, and biocompatibility, J. Polym. Res. 21 (2014) 360–375.
[33] H.Y. Wang, J.H. Ji, W. Zhang, Y.H. Zhang, J. Jiang, Z.W. Wu, S.H. Pu, P.K. Chu, Biocompatibility and bioactivity of plasma-treated biodegradable poly(butylenes succinate), Acta Biomater. 5 (2009) 279–287.
[34] M. Cerruti, S. Fissolo, C. Carraro, C. Ricciardi, A. Majumdar, R. Maboudian, Poly(ethylene glycol) monolayer formation and stability on gold and silicon nitride substrates, Langmuir 24 (2008) 10646–10653.
[35] R.N. Wenzel, Resistance of solid surfaces to wetting by water, Ind. Eng. Chem. 28 (1936) 988–994.
[36] A.B.D. Cassie, S. Baxter, Wettability of porous surfaces, Trans. Faraday Soc. 40 (1944) 546–551.